PCCP

Why does 4-biphenyl carbonyl azide have ultra-short lived excited states? An ultrafast UV–vis spectroscopic and computational study

Journal:	*Physical Chemistry Chemical Physics*
Manuscript ID	CP-ART-09-2018-005963.R1
Article Type:	Paper
Date Submitted by the Author:	05-Nov-2018
Complete List of Authors:	Peng, Huo-Lei; Albert Einstein College of Medicine, Biochemistry

Journal Name

ARTICLE

Why does 4-biphenyl carbonyl azide have ultra-short lived excited states? An ultrafast UV–vis spectroscopic and computational study

Received 00th January 20xx,
Accepted 00th January 20xx

DOI: 10.1039/x0xx00000x

www.rsc.org/

Huo-Lei Peng *[a]†

Upon excitation at 308 nm, 4-biphenyl carbonyl azide (4-BpCON$_3$) shows unusually fast decay of transient absorption associated with the first excited singlet state, with time constants of several ps in MeOH, acetonitrile, and CHCl$_3$. In cyclohexane and cyclohexene, the lifetimes are ca. 0.3 ps, which is in stark contrast to the lifetimes of hundreds of ps in the case of 2-naphthoyl azide. Furthermore, photolysis at 266 and 308 nm brought about same yields of nitrene and isocyanate products. To understand these findings we also applied ultrafast transient absorption spectroscopy to the structurally related molecule, fluorene-2-carbonyl azide (F2CON$_3$), in which the two phenyl rings are fixed in a plane by a methylene group. Both carbonyl azides (biphenyl and fluorenyl) have very short lived excited states in different solvents, indicating that the twisting of phenyl rings is not the reason for the fast decay. Theoretical studies using time dependent density functional theory (TDDFT), especially with PBE0 and CAM-B3LYP functionals, suggest that excited-state potential energy surface crossings lead to the efficient and fast decomposition of carbonyl azides upon photoexcitation. Especially, the decay of the Franck-Condon state to the S_1 state with π (**CON$_3$**)- π^*(**N$_3$'**) transition character, where -N$_3$ is in a bent conformation ($\angle$NNN=ca.125°), is the key step. Finally, a model is presented to explain solvent dependence, different decaying rates, and other experimental findings.

Introduction

Carbonyl azides have been applied to organic synthesis and photoaffinity labeling studies because they can generate two chemical reactive intermediates: isocyanates and carbonyl nitrenes upon photoexcitation.[1-3] It has shown from several ultrafast spectroscopy studies that photochemical processes of carbonyl azides usually proceed on their excited state potential surfaces, in which carbonyl nitrene and isocyanate are both formed from singlet excited carbonyl azides.[4-6] In these studies, the reported lifetimes of the first singlet excited state (S_1) are several hundred ps for 2-naphthoyl azide (2-NpCON$_3$) and tens of ps for benzoyl azide (PhCON$_3$), respectively (Fig. 1). For 4-biphenyl carbonyl azide (4-BpCON$_3$), the lifetimes are less than 5 ps. In the latter case, the short lifetimes were preliminarily attributed to the twisting of phenyl rings in the n-π^* S_2 state.[4] The different decays of excited states in those azides trigger us to ask why they behave so differently.

From the theoretical calculations in those studies, the S_1 state of t-butyl-CON$_3$, the S_4 states of 2-NpCON$_3$ and PhCON$_3$, and the S_2 state of 4-BpCON$_3$ were proposed to be dissociative.

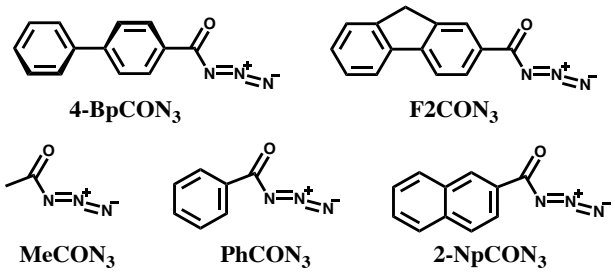

Fig. 1 Chemical structures of selected azides discussed in the text.

However, based upon product analysis and excited state studies, S_1 excitation, for example, of 4-BpCON$_3$ and 2-NpCON$_3$, clearly resulted in dissociation. Obviously, the illustration of photochemistry and photophysics of carbonyl azides based on those dissociative states is incomplete. In fact, evolution of excited carbonyl azides from the Franck-Condon state to the actual dissociative state is not clearly known. A further examination of the electronic states and the decay mechanism is much needed. In fact, several theoretical studies appeared lately to give us some insights into the dynamics of excited states of carbonyl azides.[7, 8] But those studies were focused on the non-aryl carbonyl azides.

As regards those above mentioned problems, and also to obtain a better understanding of photochemistry and photophysics of carbonyl azides, we first report a more complete ultrafast transient absorption study of 4-BpCON$_3$ and F2CON$_3$ (refer to Fig. 1). Secondly, we present an analysis of

[a] Department of Chemistry, The Ohio State University, 100 West 18th Avenue, Columbus, OH 43210, USA.
† Current address: Department of Biochemistry, Albert Einstein College of Medicine, 1300 Morris Park Avenue, Bronx, NY 10461, USA. E-mail: peng.huolei@live.com.
Electronic Supplementary Information (ESI) available: Fig. S1-S13, Table S1 for TDDFT results for selected molecules, and Scheme S1-S2 for synthesis of 2-biphenyl-5-methyl-1,3,4-oxadiazole (BpOx). See DOI: 10.1039/x0xx00000x

photolysis products and their dependence on the photoexcitation wavelength. Finally, a thorough discussion of structure and electronic properties is given according to theoretical analysis.

Experimental

Materials and Methods

All the solvents in ultrafast spectroscopy studies are spectrophotometric grade. MeOH and acetonitrile were bought from Burdick and Jackson. Cyclohexane, cyclohexene and chloroform were from Sigma-Aldrich. 4-biphenyl isocyanate, 4-biphenyl carboxamide, and other chemicals needed in synthesis, were bought from Sigma-Aldrich.

The transient absorption spectroscopy experiments were performed at Center for Chemical and Biophysical Dynamics (CCBD) in the Ohio State University. The instrumental response time is about 150-180 fs. It should be mentioned that 40-50 mL sample solution (OD = ca. 1 at the excitation wavelength or [4-$BpCON_3$]=ca.7×10^{-4} M) was kept circulating through a 1-mm CaF_2 cell in the experiments.

Photobleaching of 4-$BpCON_3$ for product analysis was achieved by excitation with 266 or 308 nm nanosecond laser (pulse width: 10-20 ns). HPLC analyses were performed on a Beckman Coulter Gold HPLC system equipped with a C18 reversed phase column(size: 250 mm×4.6 mm; particle size:5μm). 45% and 60% acetonitrile aqueous solutions were used as the mobile phase before 20 and after 21 minutes respectively. The quantities or concentrations of chemicals in the photolysis were calculated according to their peak area in HPLC chromatograms, which were corrected by samples with known concentrations.

Synthesis of carbonyl azides

1. 4-Biphenyl carbonyl azide (4-$BpCON_3$) was prepared from 4-biphenyl carbonyl chloride and NaN_3 in acetone and re-crystallized in ethyl ether. 1H-NMR ($CDCl_3$, 400 MHz): δ 8.07 (d, 2H), 7.78 (d, 2H), 7.70 (d, 2H), 7.50 (t, 2H), 7.45 (t, 1H). IR (thin film): 2177(w), 2136(vs), 1688 (st), 1607(st) cm^{-1}.

2. Fluorene-2-carbonyl azide (F2CON_3) was prepared from 2-fluorene aldehyde, NaN_3 and ICl by the procedure of Marinescu et al..[9] and followed by purification on the column chromatography ($CHCl_3$ as eluent). 1H-NMR ($CDCl_3$, 400 MHz): δ 8.17 (s, 1H), 8.05 (d, 1H), 7.82 (m, 2H), 7.58 (d, 1H), 7.39 (m, 2H), 3.93 (s, 1H). IR (thin film): 2140(st), 1675(vs), 1614(st) cm^{-1}.

The oxadiazole derivative (2-biphenyl-5-methyl-1,3,4-oxadiazole) was synthesized according the procedure (Scheme S1) described in Supplemental Information.

Computational details

All the computations were performed with ORCA 4.01.[10] Normally, def2-TZVP basis set was used in the calculations. The RIJCOSX approximation with def2/J as auxiliary basis set was employed. The ground state structures were first optimized at B3LYP/ def2-TZVP level. TDDFT with different functionals then were carried out on these structures for vertical excitations. For energy profile comparisons, the ground state structures were optimized at PBE0/ def2-TZVP level. Then vertical excitation energies and S_1 state structures (and their energies) were obtained at TD PBE0/ def2-TZVP or cam-B3LYP/ def2-TZVP level as specified in the text.

Gabedit 2.50 was used to help generate ORCA input and to monitor the progress of computations.[11] Avogadro 1.2 was used to generate molecular orbitals.[12, 13]

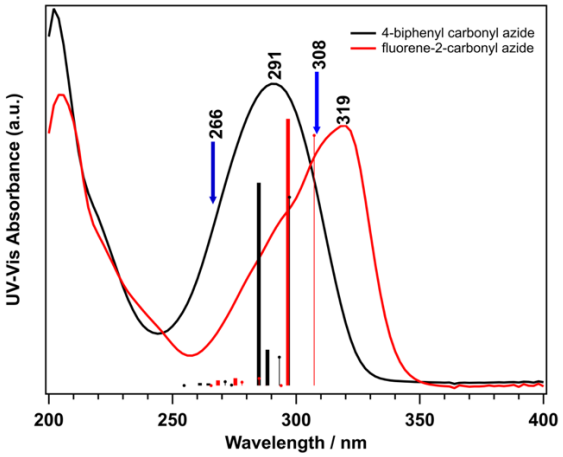

Fig. 2 UV-vis absorption spectra of 4-biphenyl carbonyl azide (4-BpCON3) and fluorene-2-carbonyl azide (F2CON3).Solvent: acetonitrile. Vertical bars are calculated electronic transitions. Thick lines for results of PBE0 functional and thin lines for results of B3LYP functional.

Results and Discussion

Ultrafast transient absorption study

In this section, we present ultrafast transient absorption studies of 4-$BpCON_3$ and F2CON_3 with 308 ± 2 nm and 270 ± 2 nm excitations in two polar solvents (MeOH (dielectric constant, ε = 33.0) and acetonitrile (ε = 36.6)) and in three less polar solvents (cyclohexane (ε = 2.02), cyclohexene(ε = 2.22), and $CHCl_3$ (ε = 4.81)).[14] According to theory (to be discussed later), 308 nm excitation promotes 4-$BpCON_3$ to the S_1 state while 270 nm excitation could lead to higher excited states (Fig. 2).

Unlike 2-$NpCON_3$, 4-$BpCON_3$ exhibits very fast decay in the ultrafast transient absorption spectra. After 308 nm excitation, 4-$BpCON_3$ shows transient absorption spectra peaking at 450-460 nm depending on the solvent (representative spectra in MeOH are shown in Fig. 3). In polar solvents such as MeOH and acetonitrile (spectra shown in Fig. 4), absorption maximums are blue-shifted around 15 nm compared to those in non-polar solvents like cyclohexane (spectra shown in Fig. 5) and cyclohexene (Fig. S1), which should be a result of stabilization of excited carbonyl azides by polar solvents. One can see that changes of λ_{max} in their decay associated spectra in polar solvents are also larger, 9 nm for MeOH and 7 nm for acetonitrile respectively, than those in chloroform where about a 5 nm difference was observed. According to TDDFT calculations, excitation at 308 nm would raise 4-$BpCON_3$ to its S_1 state. So the carrier of the transient absorption band is

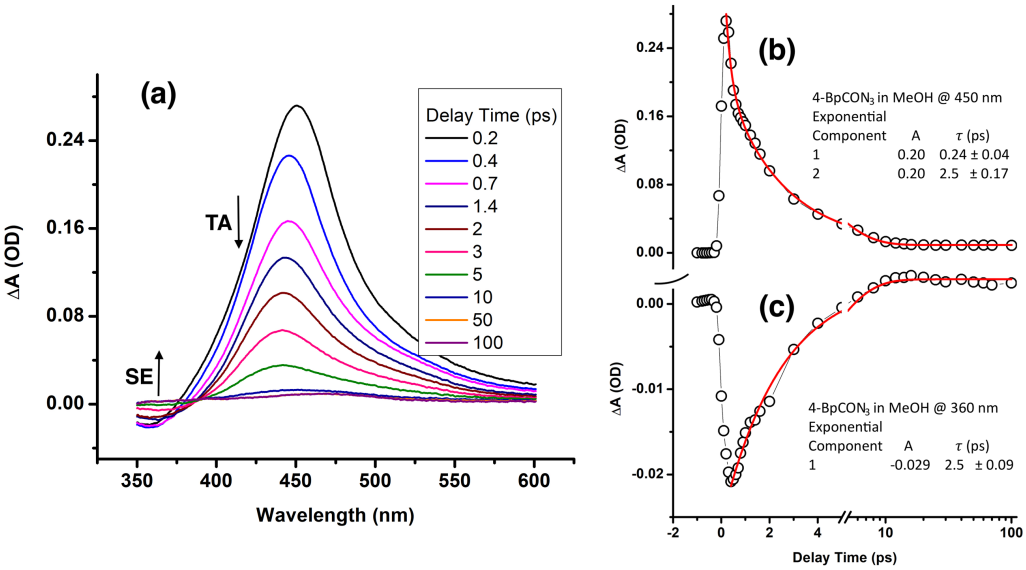

Fig. 3 Transient absorption spectra of 4-BpCON$_3$ in MeOH after 308 nm excitation (a) and selected time courses at 450 nm for transient absorption (TA) (b) and at 360 nm for stimulated emission (SE) (c) respectively.

assigned to S_1 state. Its decay was fitted with one or two exponentials with lifetimes of sub ps and 2-5 ps respectively. A weak stimulated emission (SE) at around 360 nm with lifetimes of ca. 2 ps was also observed in MeOH and acetonitrile. The lifetimes are consistent with the longer lifetimes of transient absorption. Those results are summarized in Table 1. Basically, the fast component of the decaying traces could be attributed to solvent relaxation and vibrational cooling of the S_1 state in the Franck-Condon region. At longer times one observes decay of the relaxed S_1 state.

In acetonitrile, the transient absorption spectra produced from 4-BpCON$_3$ exhibit an extra absorption band at ca. 505 nm (see Fig. 4). We confirmed that this band is due to the secondary excitation of a photolysis product, 4-biphenyl oxadiazole (BpOx), from transient absorption studies of synthesized BpOx, BpNCO and BpCONH$_2$ (refer to Fig. S2-S4 for their transient absorption spectra in SI), where only BpOx shows transient absorption peak at ca. 505 nm. Moreover, UV-vis absorbance at 308 nm of latter compounds is nearly zero (Fig. S5), whereas BpOx has significant absorbance that could result in the secondary excitation. Another special observation in acetonitrile is that the decay of transient absorption only exhibits the longer exponential component. However, it is likely the absence of the short component is due to the secondary excitation of BpOx as well.

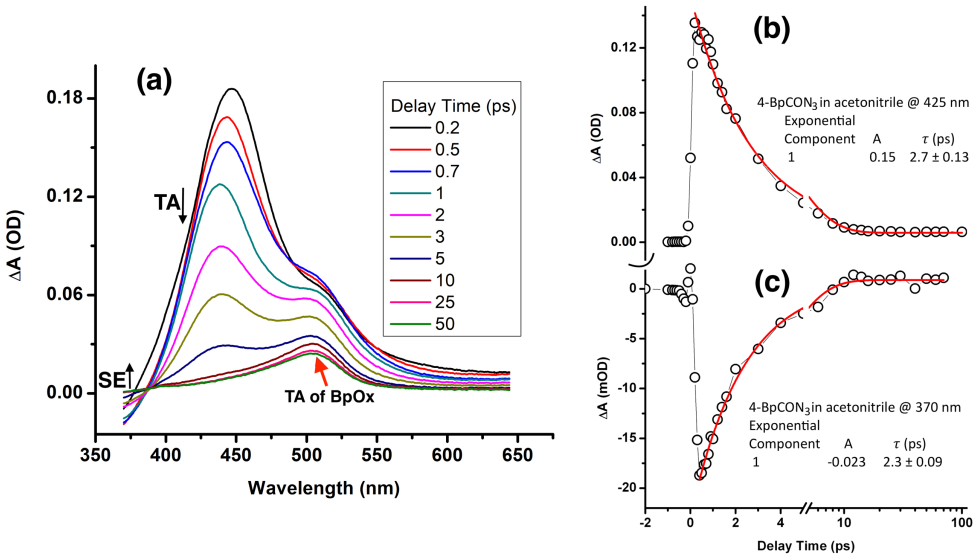

Fig. 4 Transient absorption spectra of 4-BpCON$_3$ in acetonitrile after 308 nm excitation (a) and selected time courses at 425 nm for transient absorption (TA) (b) and at 370 nm for stimulated emission (SE) (c) respectively. The red arrow in (a) points to the transient absorption of 4-Biphenyl oxadiazole (BpOx).

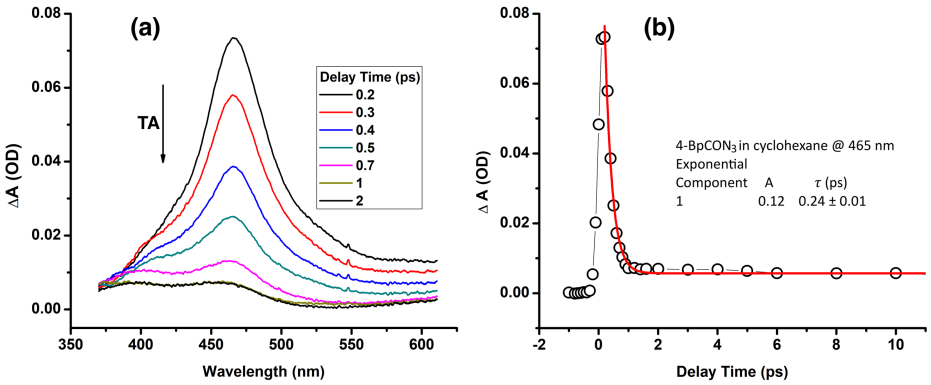

Fig. 5 Transient absorption spectra of 4-BpCON$_3$ in cyclohexane after 308 nm excitation (a) and time course at 465 nm for transient absorption (TA) (b).

Table 1 . Decay fits of transient absorption results of 4-BpCON3 after 308 nm excitation.

Solvent	SE	TA		λ_{max} (nm)[a]
	τ (ps)	τ_1 (ps)	τ_2 (ps)	
MeOH	***2.5*** *±0.09*	0.24 ± 0.04	2.5 ± 0.17	451/442
Acetonitrile	***2.3*** *±0.09*	—	2.7 ± 0.13	447/440
Cyclohexane		0.24 ± 0.01	—	467
Cyclohexene		0.34 ± 0.03	—	468
$CHCl_3$ (EtOH)		0.42 ± 0.05	5.2 ± 0.21	466/461
$CHCl_3$ (amylene)		0.95 ± 0.13	4.9 ± 0.90	466/461

[a]At 0.2 (or 0.3) and 2 (for MeOH and Acetonitrile) or 5 ps (for $CHCl_3$, in which EtOH or amylene was added as stabilizer) respectively. SE: stimulated emission; TA: transient absorption.

Striking results were found in the transient absorption (TA) in cyclohexane (Fig. 5) and cyclohexene (Fig. S1). The TA decays very fast and only an ultrashort decaying component (ca. 0.3 ps; Table 1) is observed. Such ultrafast decay is unusual and is in sharp contrast to the much slow decay observed in the case of 2-NpCON$_3$ in cyclohexane and in other non-polar solvents, like CCl_4, whereas in polar solvents like acetonitrile and MeOH, the decay of the first excited state is faster.

The lifetimes of TA of 4-BpCON$_3$ in chloroform in this study (refer to Fig. S6) are in good agreement with those reported in a previous time-resolved IR study with 270 nm excitation.[4] The decays in two $CHCl_3$ solvents are slower than those either in more polar solvents or in less polar solvents (see Table 1). So the polarity of solvent simply cannot account for the observation. Furthermore, from the steady UV-vis absorption spectra (Fig. S7), it was found in $CHCl_3$ the absorption is peaking at 295 nm, which is red-shifted in comparison to those in MeOH (292 nm), acetonitrile (291 nm), and cyclohexane (288 nm). In this regard, it is highly possible that some interactions between 4-BpCON$_3$ and $CHCl_3$ may exist, for example, the formation of a complex between the two molecules, since $CHCl_3$ has been known to form hydrogen bonds with electron donors.[15-17] We

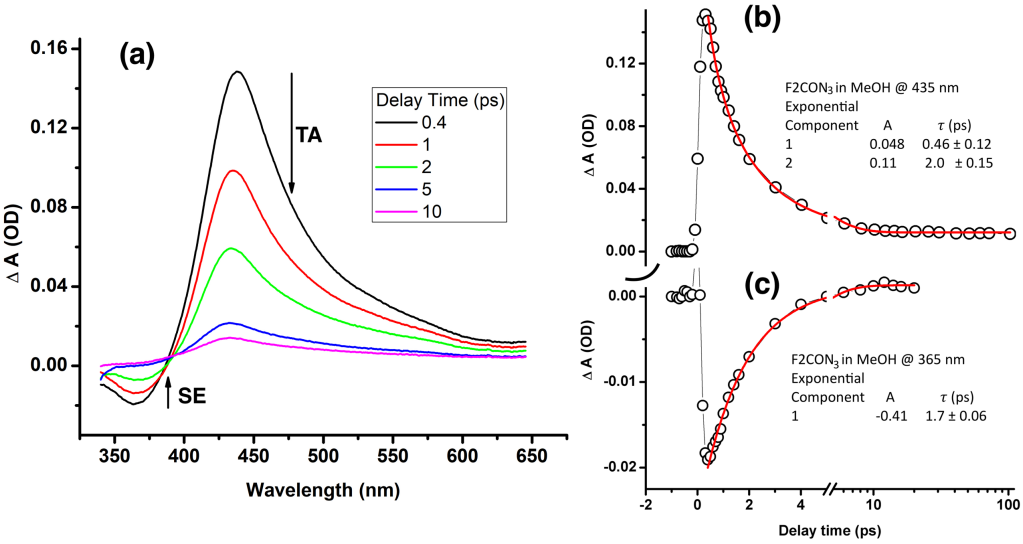

Fig. 6 Transient absorption spectra of F2CON$_3$ in MeOH after 308 nm excitation (a) and selected time courses for transient absorption (TA) at 435 nm (b) and stimulated emission (SE) at 365 nm (c) respectively.

Table 2. Decay fits of transient absorption results of $F2CON_3$ after 308 nm excitation.

Compound	Solvent	SE	TA	
		τ (ps)	τ_1 (ps)	τ_2 (ps)
$F2CON_3$	MeOH	*1.7 ± 0.06*	0.46 ± 0.12	2.0 ± 0.15
	acetonitrile	*1.2 ± 0.08*		0.91 ± 0.03

suggest hydrogen bonding between $CHCl_3$ and the excited states of 4-$BpCON_3$ is present.

Upon 270 nm excitation, 4-$BpCON_3$ should be populated to a S_n (n>1) state, which decays fast via internal conversion (IC) to give a hot S_1 state. The process should be dominating the decay of upper excited states (refer to the product analysis in the following section.). Accordingly, the transient absorption spectra associated with the S_1 state exhibit relatively slower growing, faster decay, and red-shifted transient absorption in comparison to TA with 308 nm excitation(refer to Fig. S8-S9 in SI). They also show clearly a long decaying component, even in MeOH (see Fig. S8). But considering that the secondary excitation of photoproducts might be quite severe at short excitation wavelengths due to the strong absorbances of the products (Fig. S7) at 270 nm, the long decaying component may be a result of the secondary excitation of photoproducts. Regarding this, full analysis was not performed here. We note, however, the appearance of TA of BpOx in acetonitrile (see Fig. S9) suggests nitrene formation during the photolysis.

To find whether the phenyl rotation in 4-$BpCON_3$ accounts for its short lived excited states, the transient absorption studies of the more rigid 2-fluorene carbonyl azide ($F2CON_3$) were performed. In $F2CON_3$, an effect of increased conjugation was observed, resulting in red-shifted UV-vis absorption. However, the dynamics of the excited states barely change. One can see that in MeOH and acetonitrile, $F2CON_3$ shows almost the same fast decay as 4-$BpCON_3$ (Table 2). The transient absorption band has moved to 435 nm (Fig. 6) and exhibits two-component decay in MeOH with lifetimes of 0.46 and 2.0 ps. In acetonitrile (Fig. S10), an one component decay fitting (0.91 ± 0.03 ps) gave satisfactory result as in the case for 4-$BpCON_3$. Stimulated emission (SE) was also observed at 365 nm and it decays with lifetimes of 1.7 ± 0.06 and 1.2 ± 0.08 ps in MeOH and acetonitrile respectively, which are comparable to the decay constants of transient absorption. But we may point out that 308 nm excitation may populate $F2CON_3$ to a higher excited state other than the S_1 state. However since SE and TA exhibit similar decaying lifetimes, it is reasonable to assume that the results presented here are due to the S_1 state or hot S_1 state as in the case of 4-$BpCON_3$ with 270 nm excitation. Nonetheless, above results suggest the fast decay in 4-$BpCON_3$ and $F2CON_3$ must be a result other than phenyl rotating in excited states.

Analysis of photolysis products

In general, photolysis of carbonyl azides will generate carbonyl nitrenes and isocyanates. Final products are dependent on solvents used in photolysis (Scheme S2 in SI). Photolysis of 4-$BpCON_3$ in acetonitrile was confirmed to produce 4-biphenyl isocyanate (BpNCO) and 4-biphenyl oxadiazole (BpOx), which is a product of reaction between 4-biphenyl carbonyl nitrene and acetonitrile (Fig. 7).

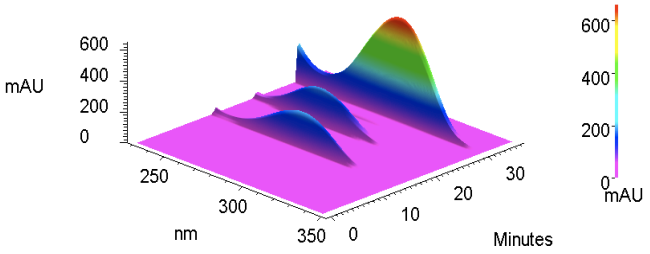

Fig. 7 3D Fractional HPLC spectra of biphenyl carbonyl azide (4-$BpCON_3$) in acetonitrile after 266 or 308 nm ns laser bleaching. The x and y axis are UV absorption wavelength and retention time respectively. EtOH was added before HPLC analysis to quench the isocyanate. The peak with the shortest retention time is assigned to BpOx. The middle peak is the 4-BpNCO ethanol adduct (Bp-NH-CO_2Et). The last fraction is unreacted 4-$BpCON_3$.

Table 3. Product yields in percentages after bleaching of 4-BpCON3 under different conditions.

Bleaching Condition	4-$BpCON_3$		Product yield (%)	
	C (mM)[a]	Decomp. %[b]	BpOx	Bp-NH-CO_2Et
308 nm, 60 mW, 5 min	9.63	50	28	52
308 nm, 60 mW, 15 min	9.63	100	24	45
308 nm, 60 mW, 15 min	1.75	100	28	62
266 nm, 116 mW, 2 min	9.63	23	24	82[c]
266 nm, 116 mW, 2 min	1.75	59	28	72
266 nm, 100 mW, 4 min	1.75	81	27	61

[a] Initial concentration of 4-$BpCON_3$.
[b] Decomposition of 4-$BpCON_3$ in percentages.
[c] The unusual high yield may be a result of reaction between azide and intermediates.

Upon photoexcitation at either 266 or 308 nm, the yield of oxadiazole (or nitrene) is around 28% (Table 3). The major photolysis product is 4-BpNCO (ca. 62%). The product yields shown in Table 3 may show some dependence on the concentration or photolysis duration but not on the excitation wavelength (for example at 1.75 mM of 4-$BpCON_3$). From the calculations, it is clear that 266 and 308 nm excitations would promote 4-$BpCON_3$ to different excited states and 308 nm excitation will produce the S_1 state directly. In this regard, we may then conclude that the photolysis proceeds in the S_1 state.

Electronic excitations in carbonyl azides

4-biphenyl carbonyl azide (4-$BpCON_3$) has a strong and broad electronic absorption in the range of 250-340 nm with a maximum at 291 nm in acetonitrile (Fig. 2). When the two phenyl rings are prevented from twisting by a methylene bridge in fluorene-2-carbonyl azide ($F2CON_3$), the UV-vis spectrum shows an unsymmetrical and red-shifted band in the same range, in which the maximum at 319 nm is on the red side (Fig.

2). Clearly, the coplanar phenyl rings in $F2CON_3$ have a notable effect on the electronic properties. In comparison to other carbonyl azides, upon looking at their UV-vis spectra, one may notice that the spectra of these two carbonyl azides are different from those of 2-naphthalene sulfonyl azide (2-$NpSO_2N_3$) and 2-naphthoyl azide (2-$NpCON_3$) (Fig. S11). For the latter two azides, weak absorption bands above 325 nm were observed. Apparently, different aryl groups have different effects on the electronic absorption of aryl substituted carbonyl azides. Since the photochemistry and photophysics of carbonyl azides are dependent on photoexcitation, understanding the origin of those absorption bands, which are associated with different electronic excited states, could help explain our observations. Especially, because of the significance of lowest excited states in the photochemistry and photophysics, we first need to know what are those states and what properties do they have, which are normally done by theoretical calculations.

For methylcarbonyl azide, the lowest excited states are associated with transitions between frontier orbitals as shown in Fig. 8. In methylcarbonyl azide ($MeCON_3$), they are π(**CA**), n(**CO**), π^*(**CA**), and π^*(**N_3**). Among these orbitals, π^*(**N_3**) is important in photodissociation because occupation of this anti bonding orbital will result in a lower bond order of -N_3, and bond breaking. When an aryl group is connected, due to the electronic interaction between the aryl group and the carbonyl azide moiety, the orbital order and the electronic transitions between those frontier orbitals may change. For example, in 4-$BpCON_3$, the orbital order is changed (Fig. 8) and aryl π orbitals are part of the frontier orbitals and contribute to transitions involving the lowest excited states. As a consequence, at the TD PBE0/ def2-TZVP level of theory, the S_1 state of 4-$BpCON_3$ is an $n\pi^*$ state (of n(**CO**)- π^* transition) and S_2 is a $\pi\pi^*$ state (of π(**Ar**)- π^* transition). This result however is different from the previous

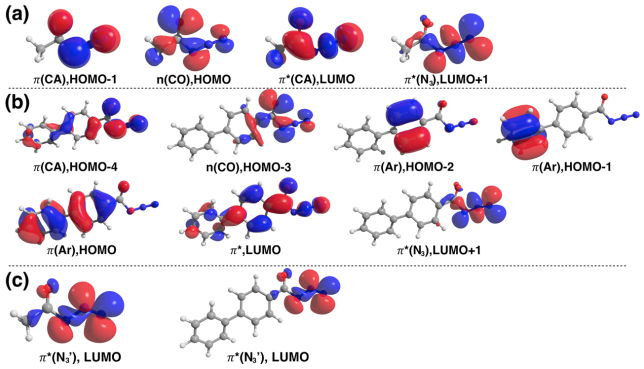

Fig. 8 Frontier orbitals of carbonyl azides related to their lowest excited state transitions. (a) $MeCON_3$ at the ground state; (b) 4-$BpCON_3$ at the ground state; (c) LUMOs of $MeCON_3$ and 4-$BpCON_3$ with bent NNN.

study, where the two lowest electronic excitations are in the reverse order at a computation level of B3LYP/TZVP. The calculated results depend on the theoretical methods employed. Furthermore, the π(**Ar**) to π^* transition, which involves in-plane electron transfer to the out-of-plane carbonyl azide moiety of π^*, clearly indicates abovementioned S_1 or S_2 states bear partial charge transfer (CT) character. Because time-dependent density functional theory (TDDFT) may underestimate CT transition energy resulting in incorrect energy levels and the wrong order of excited states, computations based on TDDFT may not be appropriate to describe these states.[18-25] Unfortunately, due to its low computational cost and simplicity, we still rely on TDDFT in many areas. For different density functionals, they may be suitable for specific molecules due to different approximations and parameterizations. In this study, at first, we need to find the best density functional for aryl substituted carbonyl azides. In doing so, theoretical

Table 4. TDDFT results of lowest electronic transitions of carbonyl azides with different density functionals. For selected calculations, oscillator strength is given in parentheses. 0.0 means the number is less than 0.001.

Theory	S_1		S_2		S_3	
	Energy (nm)	Character	Energy (nm)	Character	Energy (nm)	Character
			Molecule: 4-$BpCON_3$			
Exp. UV-vis peak	**291** (in acetonitrile)					
B3LYP	297 (0.66)	π-π^*	293 (0.099)	**n-π^***	274 (0.002)	π-π^*
PBE0	288 (0.13)	**n-π^***	285 (0.71)	π-π^*	265 (0.008)	π-π^*
CAM-B3LYP	272 (0.006)	**n-π^***	261 (1.0)	π-π^*		
ωB97x-D3	265	n-π^*	248	π-π^*		
LC-BLYP	273	n-π^*	252	π-π^*		
RI-B2PLYP	287	n-π^*	275	π-π^*	265	π-π^*
TPSS	334	π-π^*	326	n-π^*		
BLYP	346	π-π^*	337	n-π^*		
BP86	343	π-π^*	337	n-π^*		
PBE	343	π-π^*	339	n-π^*		
			Molecule: $F2CON_3$			
Exp. UV-vis peak	**319** (in acetonitrile)					
B3LYP	307 (0.87)	π-π^*	294 (0.0)	n-π^*	285 (0.025)	π-π^*
PBE0	297 (0.93)	π-π^*	288 (0.0)	n-π^*	275 (0.026)	π-π^*
CAM-B3LYP	276 (0.98)	π-π^*	272 (0.0)	n-π^*	258 (0.061)	π-π^*
RI-B2PLYP	290	π-π^*	287	n-π^*	274	π-π^*

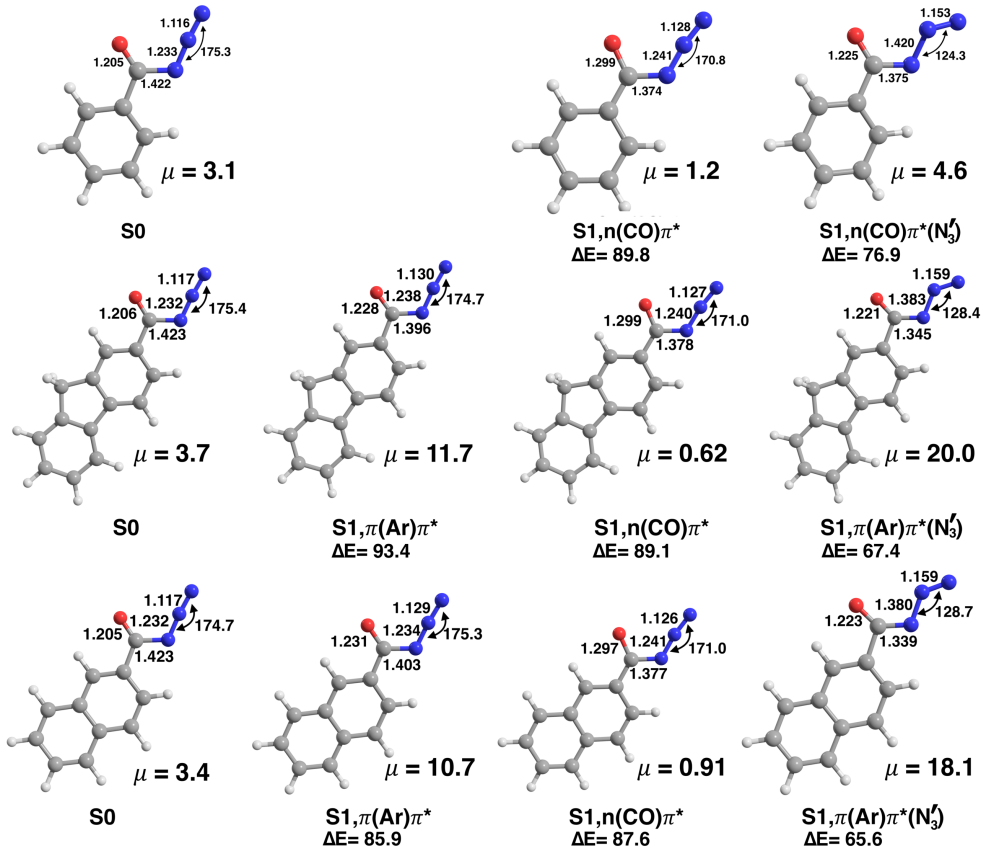

Fig. 9 Structural information of $PhCON_3$, $F2CON_3$ and $2\text{-}NpCON_3$ at their ground stats (S_0) and relaxed excited states (S_1) respectively at PBE0/ def2-TZVP level. Units: bond length, Å ;NNN angle, degrees(°). The dipole moment (μ) in Debye and ΔE, the relative energy against the ground state (S_0) in Kcal/mol are also given.

calculations with different density functionals, especially, those functionals that show better description of CT transitions like some range-separated density functionals, meta GGA, and hybrid functionals, were performed. The calculation results are summarized in Table 4 and Table S1.

From the results, one can see that the Generalized Gradient Approximation (GGA) functionals and meta-GGA: BLYP, BP86, PBE, and TPSS, are reasonably good for pure aromatic hydrocarbons: biphenyl and fluorene, but they fail on carbonyl azides. Range-separated functionals: CAM-B3LYP, ωB97x, and LC-BLYP tend to overestimate the transitions for all the compounds, especially for hydrocarbons. On the other hand, hybrid and double-hybrid functionals: B3LYP, PBE0, and B2PLYP, give the best results for carbonyl azides although they overestimate the transitions in hydrocarbons. In agreement with the previous theoretical calculations on benzoyl azide ($PhCON_3$), 2-naphthoyl azide ($2\text{-}NpCON_3$), and $4\text{-}BpCON_3$, our B3LYP calculations could confirm $4\text{-}BpCON_3$ has a ππ* S_1 state at this level. However, PBE0 and several other range-separated functionals indicate the S_1 state is largely an nπ* state with a major contribution from an n(**CO**)-π* and minor contribution from a π(**Ar**)-π* transition. In comparison, $F2CON_3$ has a ππ* S_1 state for each functionals used here. So the problem here is whether $4\text{-}BpCON_3$ has an ππ* S_1 state or an nπ* S_1 state? Seeing that $4\text{-}BpCON_3$ has a broad absorption band centered at 291 nm while $F2CON_3$ shows an absorption maximum at 319 nm and a sharp red edge. It is most likely that $F2CON_3$ has an allowed ππ* S_1 state and $4\text{-}BpCON_3$ has an nπ* S_1 state provided that B3LYP underestimate the π(**Ar**)-π* transition. However, it should be emphasized here that nπ* and ππ* states are very close energetically in $4\text{-}BpCON_3$ due to the contributions from both electronic transitions, which is also reflected in the absorption spectrum with only one overlapping band.

Calculated absorptions for other carbonyl azides with PBE0 functional also show good agreement with experimental observations. A special notice should be given to $2\text{-}NpCON_3$ since its photochemistry and photophysics have been studied in detail.[5] Its S_1 state is a π(**Ar**)-π* transition, and thus the state has CT character as well but with weak absorption. On the other hand, for $MeCON_3$ and $PhCON_3$, the S_1 state is associated with an n(**CO**)-π* transition instead. From the optimized ground state structures of carbonyl azide moiety one can see they exhibit quite similar geometries (Fig. 9). For example, on the ground state (GS) of $F2CON_3$, CO bond is 1.206 Å; C-N bond is 1.423 Å; N1-N2 and N2-N3 bonds are 1.232 and 1.117 Å respectively; and the angle of N-N-N is 175.4°, nearly linear (we will call it colinear in later discussions). $4\text{-}BpCON_3$, $PhCON_3$, $NpCON_3$, and $MeCON_3$ show almost the same structure. It looks like the interplay between the carbonyl azide moiety and

aromatic rings is not significant, especially in the ground state in these molecules.

In total, after comparing the results qualitatively and quantitatively, one may see PBE0 may be best suited for the calculations of aroyl azides. It then will be applied at first in the excited state calculations in following sections. CAM-B3LYP functional was also applied since it has been shown to have a better description of CT problem although it was also found to overestimate CT transitions.[18, 26-36] Nonetheless, qualitative conclusions could be drawn from the two types of calculations as long as their drawbacks are considered.

It should be noted, besides the two lowest excited states discussed above, excited states associated with $\pi^*(\mathbf{N_3})$ for 4-$BpCON_3$ and $F2CON_3$ are at S_5 or even higher at the PBE0/def-TZVP level. However, we may not need to know where those states are, as dissociation does not require an excitation to an excited state with character of electronic transition to $\pi^*(\mathbf{N_3})$ orbital like in 2-$NpCON_3$ (with 350 nm excitation), 4-$BpCON_3$ and $F2CON_3$ (with 308 nm excitation). Especially, when dissociation takes place, those transitions would reorder and potential energy surfaces also do crossings.

Evolution on the excited state surface

When a carbonyl azide is promoted to the S_1 excited state, it relaxes at first by vibrational cooling (VC) and solvent relaxation. It will then fall into a dissociative channel(s) which leads to N-N_2 bond fission. This simple model matches the observed bi-exponential decay of the transient signals. The decay process can be analyzed with the aid of theory.

Excited States of $MeCON_3$ Upon S_1 excitation, the initially formed excited state will have the ground state structure, according to the Franck-Condon principle. In $MeCON_3$, the S_1 state, at the ground state geometry, is an n(**CO**)π^*(**CA**) state while the S_2 and S_3 states are related to transitions to $\pi^*(\mathbf{N_3})$ orbital. Structural optimization of S_1 leads to the relaxed S_1 state with n(**CO**)π^*(**CA**) character. There are dramatic structural differences (see Fig. 10) between relaxed S_1 and S_0 as the excited state of $MeCON_3$ has a longer C=O bond (1.302 Å) and a much shorter C-N (1.345 Å) bond. The N-N-N angle is slightly bent to 172.2°. Further bending of N-N-N results in new frontier orbitals, among which the LUMO is localized on the bent N-N-N moiety. This orbital has σ character. We view this orbital as $\pi^*(\mathbf{N_3}')$ to emphasize its difference from the one with a slightly bent N-N-N group. Some researchers preferred to call this type orbital a σ^* and a state associated with this orbital, for example, $\pi\sigma^*$ state, is important in molecular photophysics.[37-41]

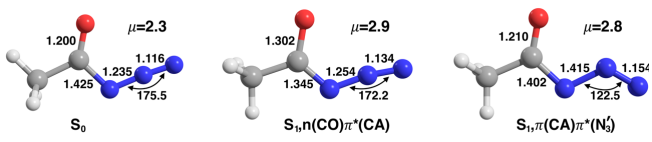

Fig. 10 Structural information of methyl carbonyl azides ($MeCON_3$) at its ground (PBE0/def2-TZVP) and relaxed excited states (CAM-B3LYP/ def2-TZVP) respectively. Dipole moment (unit: Debye) is shown on top of each structure. Angle is shown in degree (°) and bond length in Å.

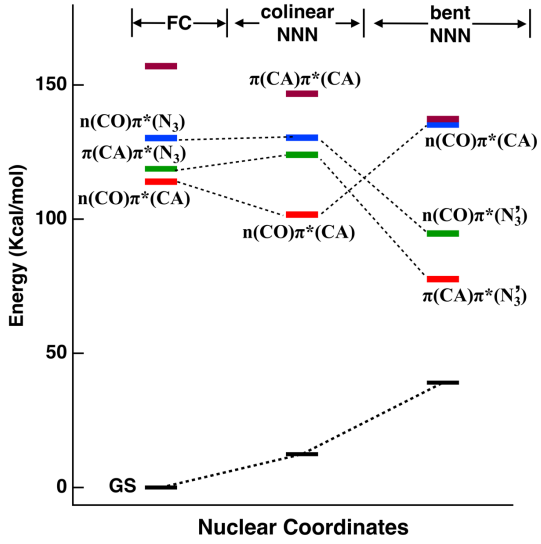

Fig. 11 CAM-B3LYP/def2-TZVP energy levels of lowest electronic states (S_0-S_4) of $MeCON_3$. The GS structures were obtained at PBE0/def2-TZVP level. The relaxed S_1 state structures were optimized at CAM-B3LYP/def2-TZVP level.

The S_1 state with π(**CA**)$\pi^*(\mathbf{N_3}')$ character exists with a much lower energy (Fig. 11). The structure associated with the state (Fig. 10) shows not only a greatly bent N-N-N angle of 122.5°, but also a long N1-N2 bond at 1.415 Å. We posit that N-N_2 fission proceeds from this bent S_1 state (π(**CA**)$\pi^*(\mathbf{N_3}')$) since it is energetically favorable in comparison to n(**CO**)π^*(**CA**) S_1 state. Later, we will show the decay on this surface is nearly barrierless.

Relaxed n(CO)π^* and π(Ar)π^* S_1 State of Aroyl Azides Replacement of the methyl group with an aryl group leads to a more complicated electronic structure. First, the LUMO of the ground state structure is a combination of π^*(**Ar**) and π^*(**CA**), which is now involved in several of the lowest excited states. Secondly, several π(**Ar**) orbitals also contribute to those transitions. As a result, excited states with $\pi^*(N_3)$ character are located at much higher energy levels. However, since excitations to the S_1 state with π(**Ar**)π^* character (e.g. in 2-$NpCON_3$ or $F2CON_3$) and with n(**CO**)π^* character (e.g. in $PhCON_3$ or 4-$BpCON_3$) both experimentally lead to N-N_2 dissociation, potential energy surface crossings among the excited states are expected after initial relaxation. Relaxation on each S_1 state surface will give rise to the relaxed π(**Ar**)π^* S_1 state and n(**CO**)π^* S_1 states respectively. In addition, we also could locate the n(**CO**)π^* S_1 state of 2-$NpCON_3$ and $F2CON_3$. Those states have different structural features (see Fig. 9) except that the bond angle of N-N-N is above 170° in all the cases, which is important to keep the electronic character with a contribution from the π^* orbital in those states.

The relaxed n(**CO**)π^* S_1 state in $PhCON_3$, 4-BpCON3, $F2CON_3$, and 2-$NpCON_3$ shows a unique carbonyl azide moiety with a longer C=O bond (ca. 1.30 Å) and a short C-N bond (less than 1.38 Å), similar to that of $MeCON_3$. The angle of N-N-N is about 4° smaller than that in GS. Such structural changes suggest the electron density is flowing out of the C=O and to part of the N_3 moiety.

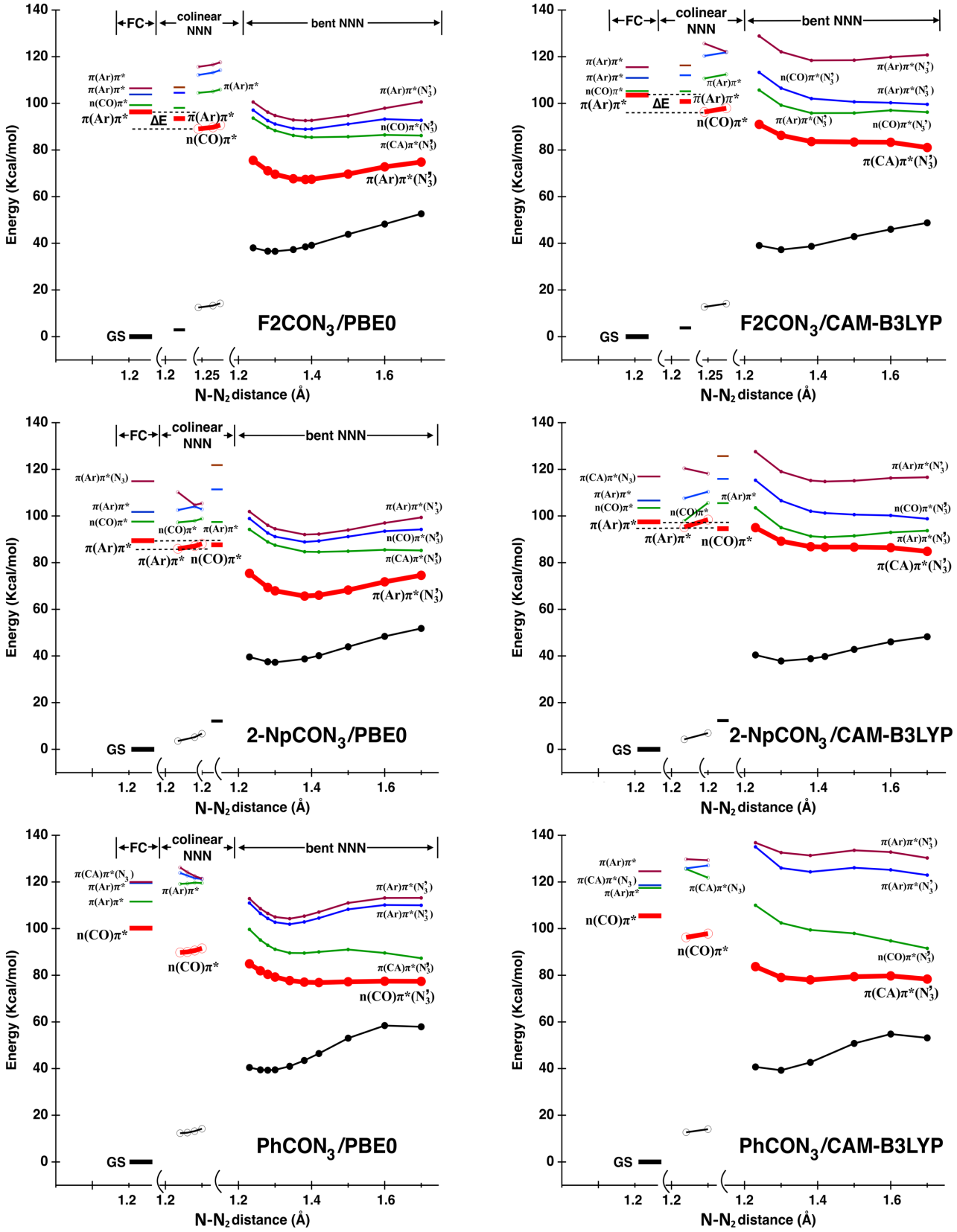

Fig. 12 Energy profiles of 5 lowest electronic states (S_0-S_4) of selected carbonyl azides at GS and S_1 state structures. The left figures are: TDDFT PBE0/def2-TZVP energies of singlet electronic states at the GS structures and the relaxed or constrained n(**CO**)π^*, π(**Ar**)π^*, and π(**Ar**)π^*(**N_3'**) (or n(**CO**)π^*(**N_3'**)) S_1 state geometries at TDDFT PBE0/def2-TZVP level. The energies of CAM-B3LYP/def2-TZVP on the structures of PBE0 are shown at the right figures. The S_1 states are shown in red. Electronic characters are given in selected states.

On the other hand, the structural changes from GS (or FC) structure to the relaxed π(**Ar**)π* S_1 are small. For example, in the state of 2-$NpCON_3$, the C=O bond is 1.231 Å and only 0.026 Å up from 1.205 Å in the GS. The C-N bond is from 1.423 to 1.403 Å; N1-N2 is from 1.232 to 1.234 Å; N2-N3 is from 1.117 to 1.129 Å; the N-N-N angle is from 174.7° to 175.3°. Consequently, small structural changes result in a much smaller energy gap on the S_1 potential energy surface between FC and the relaxed structure than that in the case of n(**CO**)π* S_1 state of $PhCON_3$ and 4-$BpCON_3$. However, since the π(**Ar**)-π* transition has charge transfer character, the dipole moment of π(**Ar**)π* S_1 state is much larger than the ground state one. Values of 10.7 and 11. 7 Debye were obtained for the state of 2-$NpCON_3$ and $F2CON_3$, respectively. On the other hand, the calculated dipole moments of the relaxed n(**CO**)π* state for $PhCON_3$ and $F2CON_3$ are 1.2 and 0.62 Debye respectively and are smaller than those in the ground state (3.1 and 3.7 Debye respectively). However, the large polarity does not bring about longer lifetimes with increasing solvent polarity as one would expect normally. In fact, previous studies indicated the relaxed state decays with lifetimes of hundreds of ps in cyclohexane and CCl_4, much longer than several tens of ps in acetonitrile and MeOH.[5] Because of the character of charge transfer (CT) in the relaxed S_1 of 2-$NpCON_3$, we suspect the reverse dependence of solvent polarity might be a result of the location of the relaxed states existing in the reversed Marcus region where more stabilization of S_1 state by polar solvent, less barrier is observed. This explanation was also applied to several studies, in which the reverse solvent dependence was also observed.[42, 43]

Excited State Decay on the S_1 State and Dissociation on the S_1 State with Bent N-N-N It is now clear the photolysis products of isocyanate and carbonyl nitrene have a common origin: the S_1 state of the carbonyl azide with different electronic characters. But it is unclear where their dissociative channels branch. Since the N1-N2 bond distance must increase along the reaction coordinates giving rise to both isocyanate and nitrene, we first tried to do a relaxed scan of N1-N2 distance on the S_1 PES. But it was not an efficient way to find the dissociation channel as there many degrees of freedom related to the carbonyl azide moiety, for example, C=O bond length, C-N bond length, the N1-N2-N3 angle, and even some dihedral angles, could strongly affect the electronic character and the energy. A full scan on these degrees will be beyond our computational resources. Also remember that the N1-N2-N3 angle is nearly collinear at the relaxed π(**Ar**)π* or n(**CO**)π* S_1 state, while a structure having a bent N1-N2-N3 on the S_1 PES is in fact energetically favored as already revealed in $MeCON_3$ (refer to Fig. 11). For aroyl azides, the bending also lowers the S_1 state energy (see Fig. 12). For example, a fully optimized $F2CON_3$ on the S_1 PES with a N-N-N angle of 128.4° is located about 20 Kcal/mol lower than its π(**Ar**)π* S_1 state in energy. Among other geometric differences from the relaxed FC structure, the distance of N1-N2 is around 1.40 Å in the structure. More importantly, the LUMO becomes π*(**N_3'**). This is a significant change since the bond fission may require an electronic transition to this orbital. Along the N1-N2 bond, the S_1 state of $PhCON_3$, $F2CON_3$, and 2-$NpCON_3$ has major character of n(**CO**)-π*(**N_3'**), π(**Ar**)-π*(**N_3'**), and π(**Ar**)-π*(**N_3'**) at

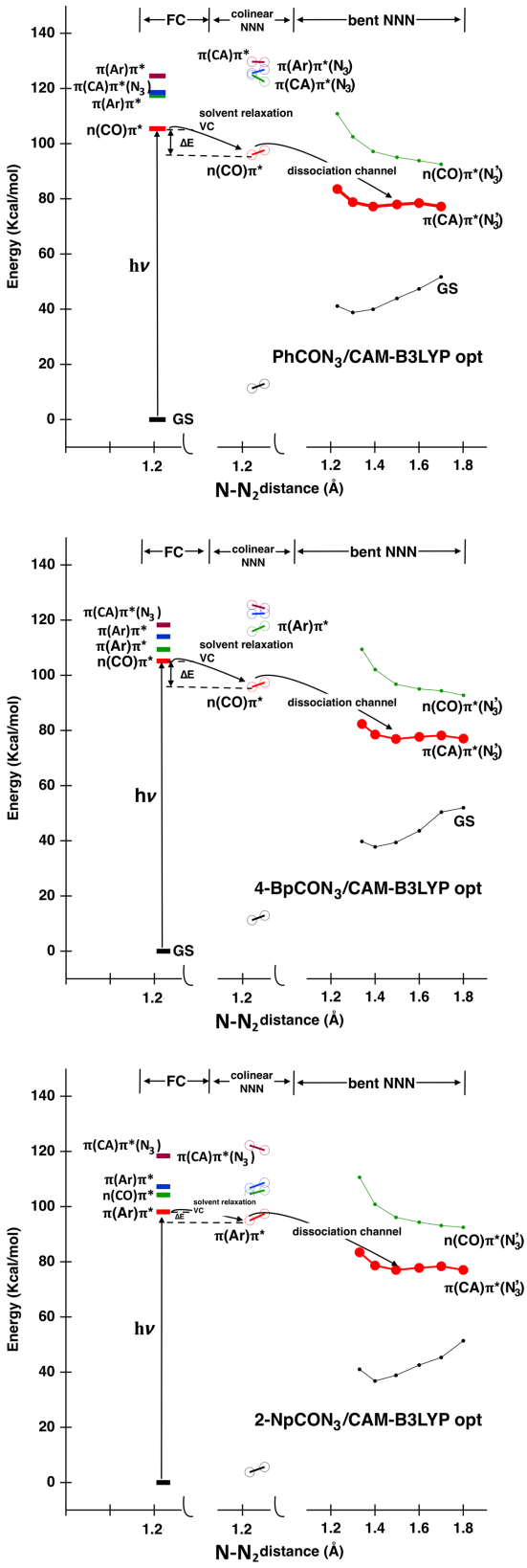

Fig. 13 CAM-B3LYP/def2-TZVP Energy profiles of the lowest electronic states (S_n (n=0-4)) of selected carbonyl azides at GS and S_1 state structures. The GS structures were obtained at PBE0/def2-TZVP level. The relaxed and constrained S_1 state structures were optimized at CAM-B3LYP/def2-TZVP level. Electronic characters are given in selected states.

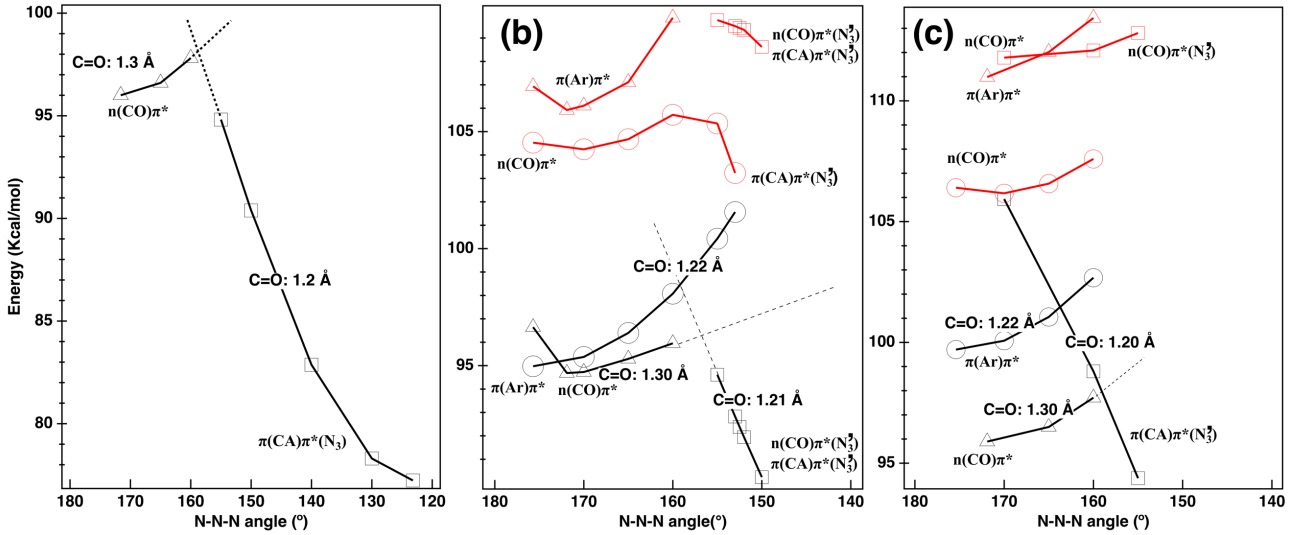

Fig. 14 Energy profiles of S_1 states (black lines and markers) along N-N-N bending. (a) $PhCON_3$; (b) $2\text{-}NpCON_3$; (c) $F2CON_3$. Square markers (☐), triangles (△) and circles (○) show results of constrained optimizations on the π(**CA**)π*(N_3') S_1 state, the n(**CO**)π* S_1 state and the π(**Ar**)π* S_1 state respectively. Red lines and markers indicate the S_2 state energies at their corresponding S_1 structures respectively.

the PBE0 level (Fig. 12). Notably, the C-N bond in the latter two azides is only about 1.34 Å, much shorter than that in other states and the state has the biggest dipole moment (refer to Fig.9). Moreover, on the π(**Ar**)π*(**N_3'**) S_1 state surface, a significant barrier was observed along with increased length of the N1-N2 bond, which may introduce another exponential in the transient decay. In addition, π(**Ar**)-π*(**N_3'**) transitions obviously have charge transfer character, for which TDDFT with the PBE0 functional will not be suitable since it underestimates charge transfer energy. To better describe these states, at least qualitatively, CAM-B3LYP density functional was thus applied to previously optimized S_1 state structures and new energies were obtained (see Fig. 12). At CAM-B3LYP/def2-TZVP level, the major transition character of S_1 (bent NNN) becomes π(**CA**)-π*(**N_3'**) and the decay becomes barrierless. Considering the aryl group in these carbonyl azides might be not a big factor in N-N_2 bond fission since non-aryl substituted carbonyl azides also show same photochemistry in certain way, the dissociative channel along the state of π(**CA**)π*(**N_3'**) will be rational. For a better comparison, the S_1 excited states of $PhCON_3$, $4\text{-}BpCON_3$, and $2\text{-}NpCON_3$ were re-optimized at cam-B3LYP/def2-TZVP level. The energy profiles are presented in Fig. 13. Although the relaxed structures (refer to Fig. S12) of π(**CA**)π*(**N_3'**) state of $4\text{-}BpCON_3$, and $2\text{-}NpCON_3$ see some changes from those optimized with the PBE0 functional (because of different electronic characters), one may see from Fig. 12 and Fig. 13, the relative energetic levels are largely kept same and the dissociation on this state is also nearly barrierless. In addition, we may also keep an eye on the relative size of dipole moments (shown in Fig. S12) in those structures of different electronic states as they are sensible to solvent polarity. Normally the order by the size of dipole moment is: π(**Ar**)π*(N_3') > π(**Ar**)π* > π(**CA**)π*(N_3') > S_0 > n(**CO**)π*.

Explanations regarding several experimental findings Up to now, we are still missing the connection between the relaxed S_1 states (n(**CO**)π* and π(**Ar**)π*) with nearly colinear N-N-N and the bent π(**CA**)π*(**N_3'**) S_1 state. Due to the multiple degrees of freedom and computational requirements, we could not find the conical intersection (CI) point or avoided crossing region; instead we only compare the energy profiles along the nuclear coordinate of N-N-N bending starting from each end state of $PhCON_3$, $2\text{-}NpCON_3$, and $F2CON_3$ (Fig. 14), from which we may extrapolate the barriers from π(**Ar**)π* to π(**CA**)π*(**N_3'**) and from n(**CO**)π* to π(**CA**)π*(**N_3'**). It appears in $2\text{-}NpCON_3$ the former (more than 3 Kcal/mol) is higher than the latter (less than 2 Kcal/mol). Also, it may be seen that the barrier from π(**Ar**)π* to π(**CA**)π*(**N_3'**) in $F2CON_3$ (less than 2 Kcal/mol) is smaller than that in $2\text{-}NpCON_3$.

In summary, from results shown in these figures, we may bring up several facts or issues that may help us to understand our experimental observations about aroyl azides.

1. n(**CO**)-π* S_1 excitation normally results in a relatively higher FC state than that of π(**Ar**)-π* excitation and a lower relaxed S_1 state. Accordingly, the relaxation also requires a larger structural change. The high energy could provide the extra driving force to escape the relaxed state, which then decays faster. Additionally, the lower barrier along the N-N-N bending from n(**CO**)π* to π(**CA**)π*(**N_3'**) S_1 state (Fig. 14), may also support the faster decay with n(**CO**)-π* S_1 excitation.
2. In contrast to n(**CO**)-π* S_1 excitation, π(**Ar**)-π* excitation has small energy difference and small structural changes during the relaxation from the FC state. This may explain that the decay ascribed to solvent relaxation and vibrational cooling upon S_1 excitation at 350 and 340 nm for $2\text{-}NpCON_3$ was not observed.

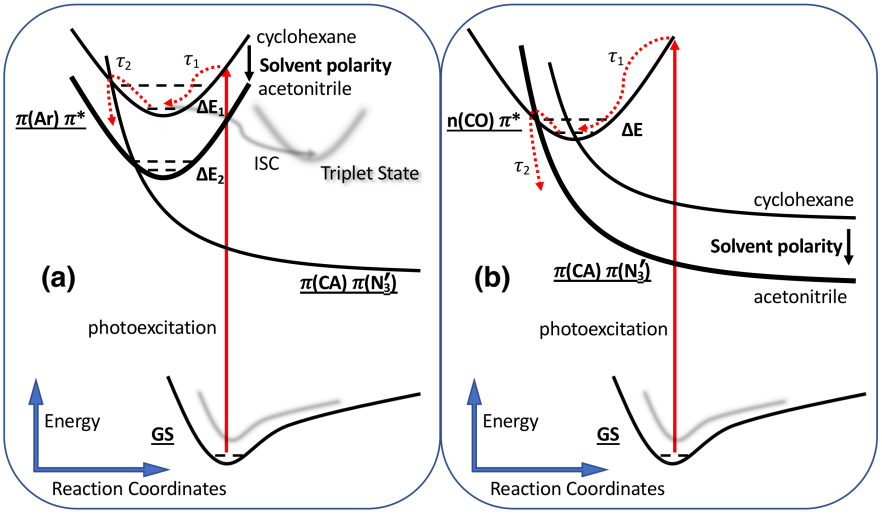

Fig. 15 Schematic potential energy surfaces of carbonyl azides and the S_1 state decay pathways.(a) Photoexcitation leads to a π(**Ar**)π^* state (like in 2-$NpCON_3$); (b) Photoexcitation leads to an n(**CO**)π^* state (like in 4-$BpCON_3$).

3. Why is the decay of excited $PhCON_3$ faster than that of excited 4-$BpCON_3$? From Fig. 12-13, one may see the energy profiles for 4-$BpCON_3$ and $PhCON_3$ are quite same since both molecules have n(**CO**)π^* S_1 state in their FC regions. However, reported results indicated that decays in $PhCON_3$ are obviously slower. By re-examination of transient IR spectra of both molecules, specifically IR bands of the S_1 state of excited azide and isocyanate, we suspect the reported larger lifetime for $PhCON_3$ could be a result of a fitting problem. The actual decaying rate for both molecules should be close instead.
4. Why does the excited 4-$BpCON_3$ decay so fast? In cyclohexane and cyclohexene, 4-$BpCON_3$ only exhibits a decaying component with a lifetime of ca. 300 fs upon 308 nm excitation. It suggests from the FC state, the excited 4-$BpCON_3$ does not have a relaxed state but falls into the dissociative channel directly.
5. Why does 2-$NpCON_3$ have a reverse solvent dependence? That is, the excited 2-$NpCON_3$ decays faster in more polar solvent like acetonitrile than does in cyclohexane or CCl_4. This is different from the findings in 4-$BpCON_3$. Keep in mind here, the S_1 state of a 2-$NpCON_3$ is π(**Ar**)π^* state and the S_1 state of 4-$BpCON_3$ is an n(**CO**)π^* state; while the dissociative S_1 state has π(**CA**)π^*(**N_3'**) character. Those different electronic characters have significant effect on their dipole moments, the order of which for those states from CAM-B3LYP calculations, is: π(**Ar**)π^* > π(**CA**)π^*(**N_3'**) > n(**CO**)π^*. Consequently, the effect of solvent polarity on their electronic energies would follow this order. In regard to this result, we introduce a simple model (presented in Fig. 15) in response to above two questions.
   In the model, photoexcitation populates the carbonyl azide into the S_1 state of π(**Ar**)π^* or n(**CO**)π^*, which is located in the converted Marcus region in relation to the dissociative S_1 state of π(**CA**)π^*(**N_3'**). In the case of π(**Ar**)-π^* excitation (Fig. 15(a)), polar solvent stabilizes π(**Ar**)π^* more than π(**CA**)π^*(**N_3'**). As a result, the energy barrier from the relaxed π(**Ar**)π^* state to π(**CA**)π^*(**N_3'**) state becomes lower when solvent polarity increases. Thus the excited state depopulates faster in polar solvents. In a nonpolar solvent like cyclohexane or CCl_4, the decay on the S_1 state surface is slow. Proportionately, the intersystem crossing (ISC) to the triplet states turn into a big factor in the decay. In addition, due to the small change from the FC state to the relaxed state, the first decay component may not be observable. On the other hand, when a carbonyl azide molecule is excited to its first S_1 state with n(**CO**)π^* character (Fig. 15(b)), it would experience a large structural change and reach a much lower relaxed n(**CO**)π^* state. Since the barrier to π(**CA**)π^*(**N_3'**) state is relatively low, the decay is normally fast. Especially, in the nonpolar solvent like cyclohexane, the barrier is gone as the more polar π(**CA**)π^*(**N_3'**) state is destabilized. In total, we can explain the solvent dependence of the decay dynamics of excited states of carbonyl azides.
6. There is one more problem we need to address. The S_1 state of $F2CON_3$, although having π(**Ar**)π^* character, decays just as fast as 4-$BpCON_3$ instead of 2-$NpCON_3$. The lower barrier of state conversion in $F2CON_3$ shown in Fig. 14 may account for that. But since the actual barrier was not obtained from our calculations, we may not exclude other possibility. From the energy profiles two findings may need to be noted. First, in $F2CON_3$, the π(**Ar**)π^* S_1 state and n(**CO**)π^* S_2 state are relatively close in energy in comparison to those states in 2-$NpCON_3$. Secondly, the FC and relaxed π(**Ar**)π^* S_1 state is energetically much higher than those in 2-$NpCON_3$ and also are much higher than the relaxed n(**CO**)π^* S_1 state in $F2CON_3$. On the other hand, in 2-$NpCON_3$, the two relaxed S_1 states are very close at energy level. With respect to these notes, if the 308 nm

excitation populates π(**Ar**)π* S_1 state of $F2CON_3$, it could perform a fast barrierless internal conversion to the n(**CO**)π* S_1 state as illustrated in Fig. S13. In such a way, the photochemistry and photophysics of $F2CON_3$ behaves like 4-$BpCON_3$. As a side note, the actual electronic character of S_1 of 4-$BpCON_3$ may be in a debate. Especially, when S_1 and S_2 (or π(**Ar**)π* and n(**CO**)π*) states are so close in energy, the order could be switched by changing solvent polarity. However, even if the S_1 state at FC region is a π(**Ar**)π* state, it still can decay very fast via a barrierless internal conversion to the n(**CO**)π* S_1 state at the first step as Fig. S13 shows.

Conclusions

In this work, we have shown that 4-biphenyl carbonyl azide (4-$BpCON_3$) and 2-fluorene carbonyl azide ($F2CON_3$) have very fast decays of excited states through ultrafast transient absorption spectroscopic studies in different solvents. The carbonyl azides generate isocyanate and carbonyl nitrene derivatives upon photoexcitation. The photochemistry takes place on the S_1 state. The rotation of phenyl rings is not a big factor in the fast photochemical and photodynamic processes. According to a series of time-dependent density functional theory (TDDFT) calculations, especially with PBE0 and CAM-B3LYP functionals, we proposed a model to explain some experimental findings. In this model, when aroyl azide molecules are populated on the S_1 state with electronic character of π(**Ar**)-π* or n(**CO**)-π*, they would look for the dissociative S_1 state with π(**CA**)-π*(**N_3'**) character, on which the N-N_2 fission is expected to take place. As those states form a reverted Marcus region, the reversed solvent dependence of π(**Ar**)π* state then could be explained since it has biggest dipole moment among those states that results in a lower barrier from the relaxed π(**Ar**)π* state to the dissociative state in more polar solvents. Similarly, the ultrafast decay of the n(**CO**)π* S_1 state in cyclohexane like in the case of 4-$BpCON_3$ is a result of small dipole moment in the state.

We may point out however, that TDDFT methods employed in this study may not be the best to describe the electronic structures of aroyl azides, considering bond breaking is involved, particularly in a quantitative perspective. With respect to this, we regard this report as a qualitative discussion. More experimental studies and theoretical methods with higher precision would be needed for the best results, especially, to find the pathway leading to the dissociative π(**CA**)π*(**N_3'**) state from the relaxed S_1 state in FC region. It is also unclear when the channels for the formation of isocyanate and carbonyl nitrene are separated on the potential energy surface although it is known they have a same origin, S_1 state of carbonyl azides. Obviously, for a full understanding of photochemistry and photophysics of carbonyl azides, we have more work to do. Nonetheless, the study in this report gave us a much needed insight into the photochemistry and physics of aroyl azides.

Conflicts of interest

There are no conflicts to declare.

Acknowledgements

The author thanks Prof. Matt Platz providing the chance to carry out the study at the Ohio State University and also appreciate his review of this manuscript and suggestions.

Notes and references

1 T. Melvin and G. B. Schuster, *Photochem. Photobiol.*, 1990, **51**, 155-160.
2 K. Ichimura, *Chem. Lett.*, 1976, **5**, 641-642.
3 E. Brachet, T. Ghosh, I. Ghosh and B. Konig, *Chem. Sci.*, 2015, **6**, 987-992.
4 S. Vyas, J. Kubicki, H. L. Luk, Y. Zhang, N. P. Gritsan, C. M. Hadad and M. S. Platz, *J. Phys. Org. Chem.*, 2012, **25**, 693-703.
5 J. Kubicki, Y. Zhang, S. Vyas, G. Burdzinski, H. L. Luk, J. Wang, J. Xue, H. L. Peng, E. A. Pritchina, M. Sliwa, G. Buntinx, N. P. Gritsan, C. M. Hadad and M. S. Platz, *J. Am. Chem. Soc.*, 2011, **133**, 9751-9761.
6 J. Kubicki, Y. Zhang, J. Wang, H. L. Luk, H. L. Peng, S. Vyas and M. S. Platz, *J. Am. Chem. Soc.*, 2009, **131**, 4212-4213.
7 X.-L. Peng, W.-L. Ding, Q.-S. Li and Z.-S. Li, *Org. Chem. Front.*, 2017, **4**, 1153-1161.
8 B. B. Xie, C. X. Cui, W. H. Fang and G. Cui, *Phys. Chem. Chem. Phys.*, 2018, **20**, 19363-19372.
9 L. Marinescu, J. Thinggaard, I. B. Thomsen and M. Bols, *J. Org. Chem.*, 2003, **68**, 9453-9455.
10 F. Neese, *Wiley Interdiscip. Rev. Comput. Mol. Sci.*, 2018, **8**, e1327.
11 A.-R. Allouche, *J. Comput. Chem.*, 2011, **32**, 174-182.
12 *Avogadro: an open-source molecular builder and visualization tool. Version 1.20. http://avogadro.cc/*.
13 M. D. Hanwell, D. E. Curtis, D. C. Lonie, T. Vandermeersch, E. Zurek and G. R. Hutchison, *J. Cheminform.*, 2012, **4**, 17.
14 C. Wohlfarth, in *CRC Handbook of Chemistry and Physics*, ed. D. R. Lide, CRC Press/Taylor and Francis, Boca Raton, Florida, USA, 90th edn., 2009, pp. 6-148-6-149.
15 A. S. R. Koti and N. Periasamy, *J. Fluoresc.*, 2000, **10**, 177-177.
16 K. Kwak, D. E. Rosenfeld, J. K. Chung and M. D. Fayer, *J. Phys. Chem. B*, 2008, **112**, 13906-13915.
17 E. Perochon, A. Lopez and J. F. Tocanne, *Chem. Phys. Lipids*, 1991, **59**, 17-28.
18 P. Wiggins, J. A. G. Williams and D. J. Tozer, *J. Chem. Phys.*, 2009, **131**, 091101.
19 Y.-L. Wang and G.-S. Wu, *Int. J. Quantum. Chem.*, 2008, **108**, 430-439.
20 S. Grimme and M. Parac, *ChemPhysChem*, 2003, **4**, 292-295.
21 D. Bousquet, R. Fukuda, P. Maitarad, D. Jacquemin, I. Ciofini, C. Adamo and M. Ehara, *J. Chem. Theory Comput.*, 2013, **9**, 2368-2379.
22 A. Acharya, S. Chaudhuri and V. S. Batista, *J. Chem. Theory Comput.*, 2018, **14**, 867-876.
23 R. J. Magyar and S. Tretiak, *J. Chem. Theory Comput.*, 2007, **3**, 976-987.
24 N. Kuritz, T. Stein, R. Baer and L. Kronik, *J. Chem. Theory Comput.*, 2011, **7**, 2408-2415.
25 C. Adamo and D. Jacquemin, *Chem. Soc. Rev.*, 2013, **42**, 845-856.
26 D. Jacquemin, V. Wathelet, E. A. Perpete and C. Adamo, *J. Chem. Theory Comput.*, 2009, **5**, 2420-2435.
27 F. J. Avila Ferrer, F. Santoro and R. Improta, *Comput. Theor. Chem.*, 2014, **1040-1041**, 186-194.
28 M. T. P. Beerepoot, D. H. Friese, N. H. List, J. Kongsted and K. Ruud, *Phys. Chem. Chem. Phys.*, 2015, **17**, 19306-19314.

29 E. Rudberg, P. Salek, T. Helgaker and H. Agren, *J. Chem. Phys.*, 2005, **123**, 184108.
30 T. Yanai, D. P. Tew and N. C. Handy, *Chem. Phys. Lett.*, 2004, **393**, 51-57.
31 H. L. Peng and R. Callender, *Photochem. Photobiol.*, 2017, **93**, 1193-1203.
32 M. A. Mosquera, C. H. Borca, M. A. Ratner and G. C. Schatz, *J. Phys. Chem. A*, 2016, **120**, 1605-1612.
33 R. Improta, F. Santoro and L. Blancafort, *Chem. Rev.*, 2016, **116**, 3540-3593.
34 M. V. Bohnwagner, I. Burghardt and A. Dreuw, *J. Phys. Chem. A*, 2016, **120**, 14-27.
35 A. Chrostowska, S. Xu, A. Maziere, K. Boknevitz, B. Li, E. R. Abbey, A. Dargelos, A. Graciaa and S. Y. Liu, *J. Am. Chem. Soc.*, 2014, **136**, 11813-11820.
36 E. Berardo, H. S. Hu, H. J. van Dam, S. A. Shevlin, S. M. Woodley, K. Kowalski and M. A. Zwijnenburg, *J. Chem. Theory Comput.*, 2014, **10**, 5538-5548.
37 K. A. Zachariasse, S. I. Druzhinin, S. A. Kovalenko and T. Senyushkina, *J. Chem. Phys.*, 2009, **131**, 224313.
38 M. Z. Zgierski, T. Fujiwara and E. C. Lim, *Acc. Chem. Res.*, 2010, **43**, 506-517.
39 T. Fujiwara, M. Z. Zgierski and E. C. Lim, *Phys. Chem. Chem. Phys.*, 2011, **13**, 6779-6783.
40 T. Fujiwara, J. K. Lee, M. Z. Zgierski and E. C. Lim, *Phys. Chem. Chem. Phys.*, 2009, **11**, 2475-2479.
41 M. Z. Zgierski and E. C. Lim, *J. Chem. Phys.*, 2005, **122**, 111103.
42 Y. T. Kao, X. Guo, Y. Yang, Z. Liu, A. Hassanali, Q. H. Song, L. Wang and D. Zhong, *J. Phys. Chem. B*, 2012, **116**, 9130-9140.
43 B. Dereka, D. Svechkarev, A. Rosspeintner, M. Tromayer, R. Liska, A. M. Mohs and E. Vauthey, *J. Am. Chem. Soc.*, 2017, **139**, 16885-16893.

TOC

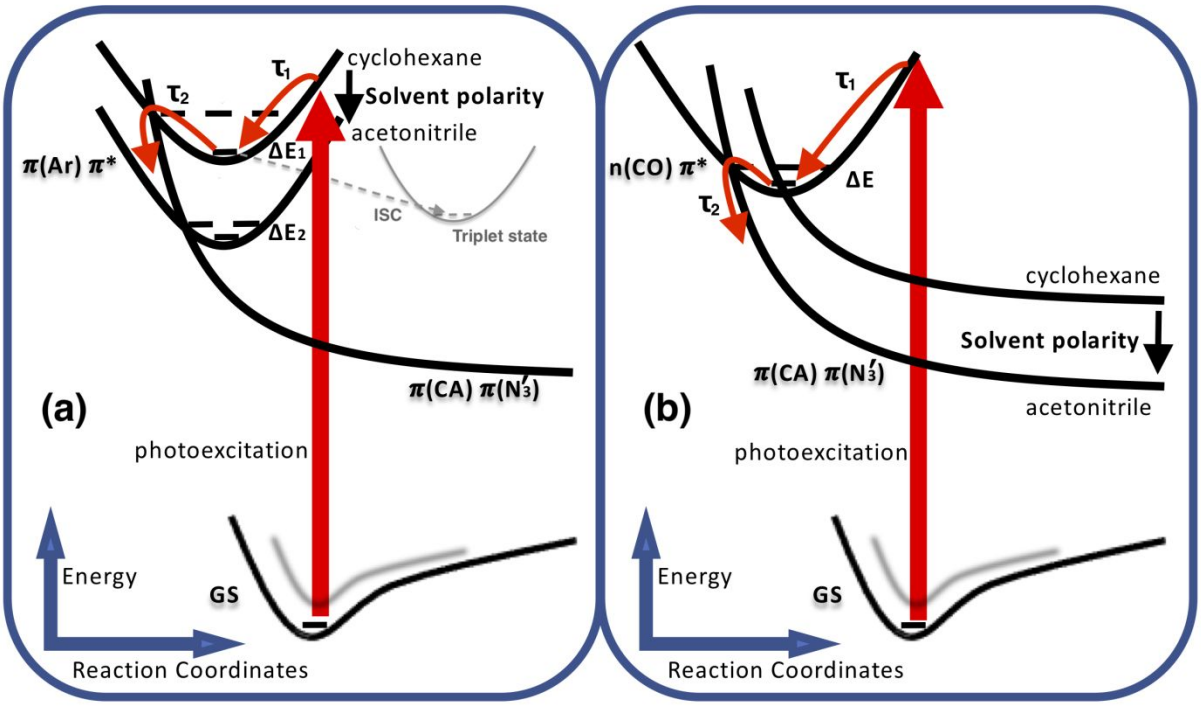

A new model is presented for ultrashort-lived excited states of carbonyl azides, their solvent dependence and other experimental observations.